

Phase morphology, thermomechanical, and crystallization behavior of uncompatibilized and PP-g-MAH compatibilized polypropylene/polystyrene blends

Jyotishkumar Parameswaranpillai,¹ George Joseph,¹ Seno Jose,² Nishar Hameed³

¹Department of Polymer Science and Rubber Technology, Cochin University of Science and Technology, Cochin 682022, Kerala, India

²Department of Chemistry, Government College Kottayam, Kerala, India 686013

³Institute for Frontier Materials, Carbon Nexus, Deakin University, Waurn Ponds Campus, Geelong, VIC, 3220, Australia

Correspondence to: J. Parameswaranpillai (E-mail: jyotishkumarp@gmail.com)

ABSTRACT: In this article, we discuss the phase morphology, thermal, mechanical, and crystallization properties of uncompatibilized and compatibilized polypropylene/polystyrene (PP/PS) blends. It is observed that the Young's modulus increases, but other mechanical properties such as tensile strength, flexural strength, elongation at break, and impact strength decrease by blending PS to PP. The tensile strength and Young's modulus of PP/PS blends were compared with various theoretical models. The thermal stability, melting, and crystallization temperatures and percentage crystallinity of semicrystalline PP in the blends were marginally decreased by the addition of amorphous PS. The presence of maleic anhydride-grafted polypropylene (compatibilizer) increases the phase stability of 90/10 and 80/20 blends by preventing the coalescence. Hence, finer and more uniform droplets of PS dispersed phases are observed. The compatibilizer induced some improvement in impact strength for the blends with PP matrix phase, however fluctuations in modulus, strength and ductility were observed with respect to the uncompatibilized blend. The thermal stability was not much affected by the addition of the compatibilizer for the PP rich blends but shows some decrease in the thermal stability of the blends, where PS forms the matrix. On the other hand, the % crystallinity was increased by the addition of compatibilizer, irrespective of the blend concentration. © 2015 Wiley Periodicals, Inc. *J. Appl. Polym. Sci.* **2015**, *132*, 42100.

KEYWORDS: properties and characterization; structure-property relations; thermal properties; thermogravimetric analysis (TGA); thermoplastics

Received 20 September 2014; accepted 9 February 2015

DOI: 10.1002/app.42100

INTRODUCTION

Polymer blending is a simple approach to develop new polymeric materials having a variety of commercial applications. The important advantage of polymer blending is that the properties of the blends can be manipulated according to the end use by the proper selection of component polymers. Polypropylene (PP) and polystyrene (PS) are the two most widely used commercial polymers. The properties of the polymer blend systems are affected by phase morphology to a greater extent. The morphology depends on the composition, viscosity ratio, interfacial tension between the blend components and also the processing condition.^{1,2} Since PP/PS blends are highly immiscible due to the non-polar nature of the polymers, their blends are highly incompatible too. Thus PP/PS blends exhibit an unstable, coarse morphology in the molten state due to high interfacial tension derived from unfavorable interfa-

cial interactions, accompanied by poor interfacial adhesion on solidification. A considerable amount of work on compatibilizing PP and PS has been done in the past by adding block or graft compatibilizer.^{2–13} In general, the compatibilizer enhances the interfacial adhesion between the phases, provides stabilization against phase coarsening leading to finer dispersion of minor phase there by decreases the interfacial tension. Another method of compatibilization is by adding reactive compatibilizer that reacts with the component polymers during the melt mixing stage to form chemical bonds between them.^{14,15} Besides the direct addition, compatibilizer can be produced by *in situ* reaction.¹⁶ Recently, it has been reported that nano fillers are also used as compatibilizers.^{17–19}

For the fabrication of polymeric materials for specific applications, a detailed understanding of thermo-mechanical properties

Additional Supporting Information may be found in the online version of this article.

© 2015 Wiley Periodicals, Inc.

of polymers is very important. Superior thermal stability of the blends of ethylene-methyl acrylate (EMA) copolymer and polydimethylsiloxane rubber (PDMS) was reported by Santra *et al.*²⁰ According to the authors, 30 : 70 EMA/PDMS blend was found to be the most thermally stable. In an interesting study, Omorov *et al.* used fractional or bulk crystallization behavior of crystallizable PP phase in the PP/PS blends to identify the matrix/droplet or co-continuous phase morphology, and established a close relationship between crystallization behavior of PP and morphology.¹ Jose *et al.* have studied the effect of blend ratio on phase morphology, crystallization behavior and mechanical properties of PP/High-density polyethylene (HDPE) blends.²¹ They found that the morphology has a profound effect on the thermo-mechanical properties, which in turn depends on the blend ratio. Horak *et al.* successfully developed high impact PP/PS blends by compatibilizing with styrene-butadiene-styrene (SBS) triblock copolymer.²² Very recently, blends of PP/HDPE with and without compatibilizer (ethylene propylene diene monomer rubber (EPDM)) were studied by Jose *et al.* and reported improvement in mechanical properties by the addition of compatibilizer.²³ Even though PP/PS blends exhibit relatively low impact strength,²⁴ only a few studies were reported to improve the mechanical properties of these blends using maleic anhydride-grafted polypropylene (PP-g-MAH) as compatibilizer. In an earlier work, we have reported on the compatibility and viscoelastic properties of PP/PS blends in the presence and absence of PP-g-MAH.²⁵ The study revealed that compatibilization has a profound effect on the morphology and viscoelastic properties of the blends. Therefore it is very important to correlate the morphology of the blends with thermo-mechanical and crystallization properties, in the presence and absence of PP-g-MAH. In this article, the thermal, mechanical and crystallization properties of PP/PS blends were systematically studied with and without compatibilizer and correlated with the morphology.

EXPERIMENTAL

Materials and Preparation of Blends

Polypropylene (PP) grade 1110 MAS having density 0.9 g/cm^3 was supplied by Indian Oil Corporation. Polystyrene (PS), grade POLYSTYROL 147F GR21, having density 1.05 g/cm^3 was supplied by Styrolution India Private Ltd. Compatibilizer used was polypropylene-graft-maleic anhydride (PP-g-MAH) with 8 to 10 wt % MAH. PP-g-MAH was obtained from Sigma Aldrich. PP/PS blends were prepared by melt mixing, using Thermo Haake PolyLab QC system equipped with roller rotors. The mixing was done at 180°C with a rotor speed of 50 rpm for 8 min. For making compatibilized blends, PP and PS were melt mixed for 2 min, followed by the addition of the compatibilizer and the mixing was continued for another 6 min. The resulting blends were hot pressed into sheets and cut in to pieces and injection molded in a DSM explore, Micro 12cc injection molding machine at 190°C , for preparing test specimens for impact, tensile, and flexural testing as per relevant ISO standards. A series of PP/PS blends were prepared and named as neat PP (100/0), 90/10, 80/20, 70/30, 60/40, 50/50, 40/60, 30/70, 20/80, 10/90, and neat PS (0/100) depending on the weight % of the component polymers.

Characterization

Scanning Electron Microscopy (SEM). The morphology of the blend materials was examined with a JEOL NeoScope JCM 5000 SEM (Japan) at an acceleration voltage of 10 kV at high vacuum. The cryo-fractured surfaces were coated with thin layers of gold before the observation.

Thermogravimetric Analysis (TGA). The thermal stability of the polymer blends was analyzed using a TGA-Q-50 TA instrument in nitrogen atmosphere with flow rate of 40 mL/min. The sample weight of about 5 to 7 mg was used and test was carried out from room temperature to 600°C at a heating rate of $20^\circ\text{C}/\text{min}$.

Differential Scanning Calorimetry (DSC). Thermal properties were determined using Mettler Toledo DSC 822e differential scanning calorimetry. The parameters such as crystallization temperature (T_c), melting temperature (T_m), total enthalpy of crystallization (ΔH_c), total enthalpy of fusion (ΔH_f), and percentage crystallinity (X_c) are derived from the DSC thermogram. Samples of approximately 10 mg were placed into ceramic pans and the tests were performed in a dry nitrogen atmosphere (flow rate of 20 mL/min). The heating was done from -50 to 200°C at a heating rate of $10^\circ\text{C}/\text{min}$, followed by cooling at $10^\circ\text{C}/\text{min}$. The melting and crystallization were determined from the DSC heating and cooling curves. ΔH_f and ΔH_c were obtained from the areas under the melting and crystallization peaks. Indium and silver samples were used as calibration standards.

The percentage crystalline content (X_c) was determined using eq. (1):

$$X_c = \frac{\Delta H}{\Delta H_{\max} \times W_{\text{poly}}} \times 100 \quad (1)$$

where ΔH is the total enthalpy of melting, ΔH_{\max} is the enthalpy of melting for a theoretically 100% crystalline polymer and W_{poly} is the weight fraction of a polymer in the blend. The term ΔH_{\max} is a reference value and represents the enthalpy of fusion of 100% crystalline polymer, which is taken as 207.1 J/g , for PP.

Mechanical Studies. The tensile properties of the samples were measured using a universal testing machine (Tinius Olsen) model H 50 KT at a cross head speed of 50 mm/min. according to ISO 527 on dumbbell shaped specimens. The sample dimensions were $75 \times 5 \times 2 \text{ mm}^3$. The span length used was 55 mm. Flexural strength of the blends were measured using a universal testing machine (Tinius Olsen) model H 50 KT, according to ISO 178, using sample dimensions $80 \times 10 \times 4 \text{ mm}^3$. The span length used was 50 mm. The testing was done at a cross-head speed of 10 mm/min. Impact testing was carried out according to ISO 180 using a Resil impactor junior. The sample dimensions were $80 \times 10 \times 4 \text{ mm}^3$.

RESULTS AND DISCUSSION

Uncompatibilized Blends

Phase Morphology. Figure 1 shows the scanning electron micrographs of the PP/PS blends at different blend ratios. Pure PP is homogeneous with rough patterns, typical characteristics of tough

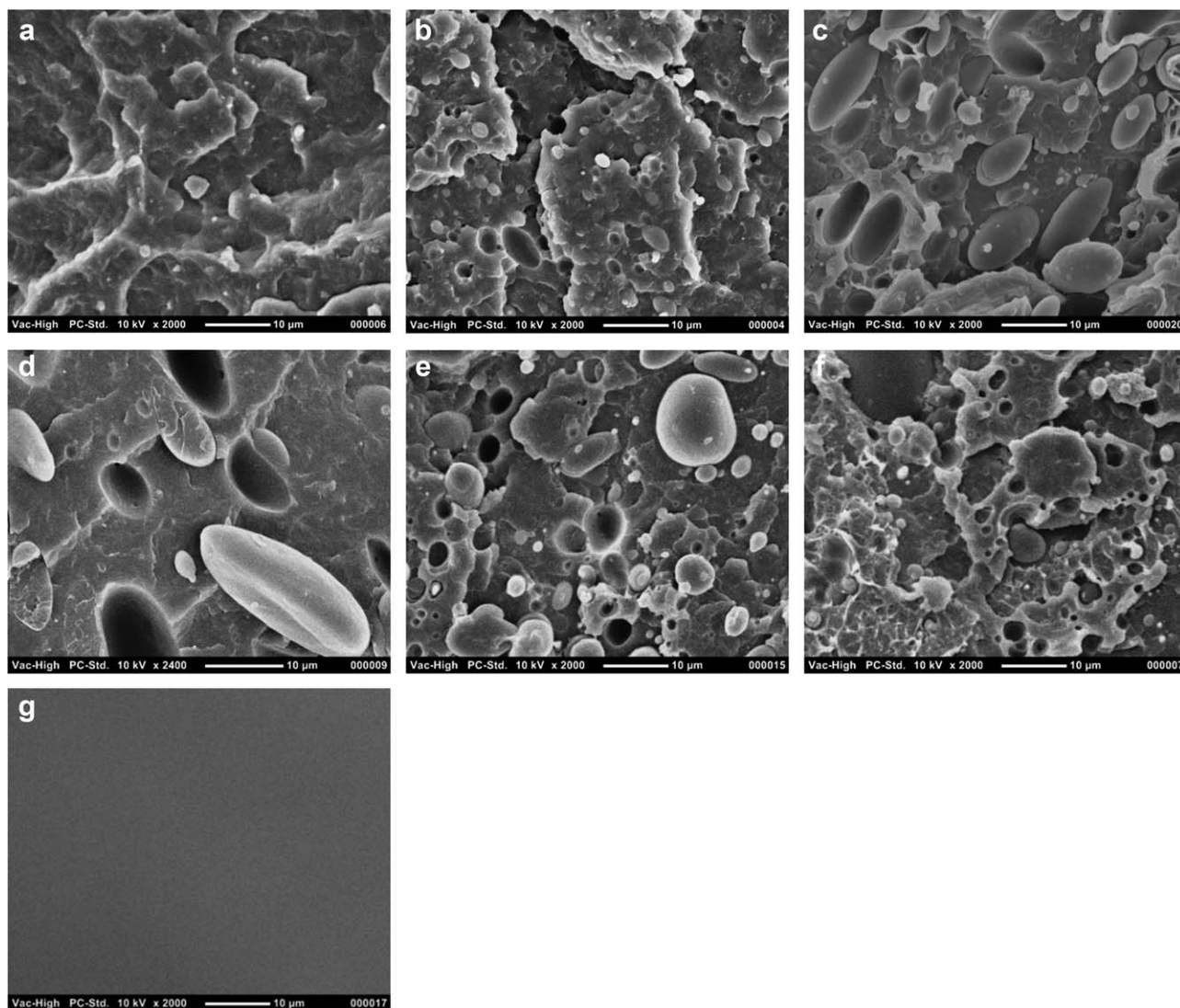


Figure 1. SEM micrographs showing the morphology of PP/PS blends.

fracture as revealed by Figure 1(a). For 90/10, [Fig. 1(b)] 80/20 [Fig. 1(c)] and 60/40 [Fig. 1(d)] blends, the PP phase formed the matrix and the PS the domains. The size of the PS domains increases with increasing concentration of the PS phase due to coalescence during the melt mixing stage.²⁶ For 40/60 [Fig. 1(e)] and 20/80 [Fig. 1(f)], phase inverted structures are observed in which PP is dispersed in the PS matrix. It can be seen from the SEM micrographs that most of the domains are removed out of the matrix phase, due to the poor interfacial adhesion between the phases.⁸ Neat PS [Fig. 1(g)] exhibits a flat homogeneous surface.

Thermogravimetric Studies. Thermal stability of the PP/PS blends was studied using TGA, in nitrogen atmosphere. The TGA and DTA profiles of polymer blends are shown in Figure 2(a,b). Thermal stability can be expressed in terms of parameters like initial decomposition temperature (T_i), maximum decomposition temperature (T_{max}), and final degradation temperature (T_f). The values obtained for T_b , T_{max} , and T_f from the thermograms are presented in Table I. The T_b , T_{max} , and T_f of PP reduced from 439, 471, 487 to 407, 435, 451, respectively, by the addition of 80 wt %

PS. This means that T_b , T_{max} , and T_f of the blends decrease with PS addition; neat PP shows the maximum thermal stability and neat PS shows the minimum. The thermal stability of the polymer blends is in between neat PP and neat PS and decreases gradually with the addition of the PS phase, which means that the blend ratio has a strong effect on the thermal stability of the polymer blends. In other words, the phase morphology plays an important role in determining the thermal stability of the blends. It should be noted that in 90/10, 80/20 and 60/40 blends, PP is the matrix phase, thus in these blends, the thermal degradation of PS phase is suppressed, since PP matrix offers thermal protection to the dispersed PS domains. On the other hand, for 20/80 and 40/60 blends, PS forms the matrix and PP the dispersed phase. As a result, the PS phase is more susceptible to thermal degradation. T_b , T_{max} , and T_f of PS are much lower than those of neat PP and the difference in T_b , T_{max} , and T_f between pure PP and pure PS are 39, 39, and 41°C respectively.

Melting and Crystallization Behavior of PP/PS Blends. Melting and crystallization of PP/PS blends were analyzed using

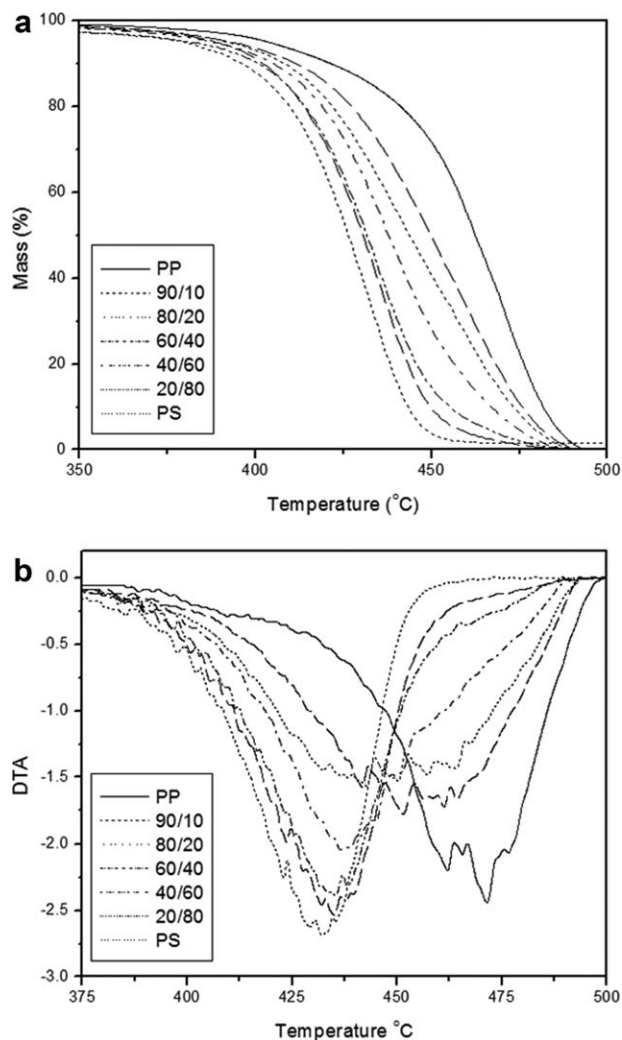


Figure 2. Effect of blend ratio on the thermograms of PP/PS blends (a) TGA (b) DTA.

DSC. The DSC heating and cooling curves are shown in Figure 3(a,b). The important parameters such as T_g , T_m , ΔH_c , ΔH_f , and X_c were derived from the DSC heating and cooling curves and are given in Table II. The T_m of PP was found to be 165.5°C, whereas T_c of PP was observed at 126.6°C. From the table, it is seen that the blend ratio/phase morphology has a strong effect on the T_m and T_c of PP. The T_m and T_c of PP are slightly reduced for the blends; the T_m of PP decreased from

Table I. Effect of Blend Ratio on the T_b , T_{max} , and T_f of PP/PS Blends

Samples (PP/PS)	T_i (°C)	T_{max} (°C)	T_f (°C)
100/0 (PP)	439	471	487
90/10	418	451	483
80/20	411	442	478
60/40	409	438	466
40/60	407	435	455
20/80	407	435	451
0/100 (PS)	400	432	446

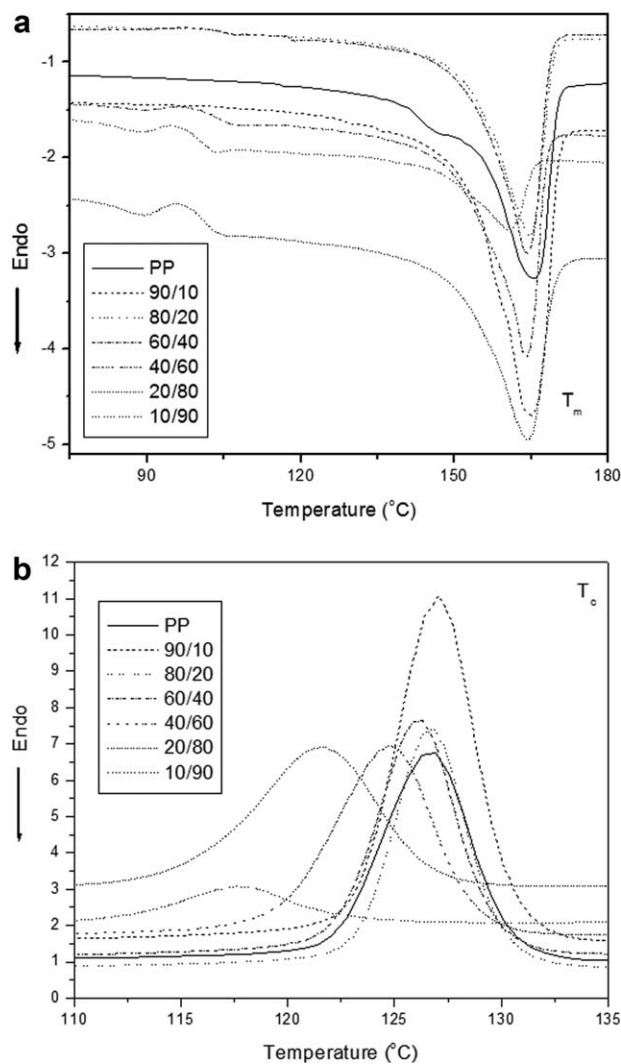


Figure 3. a. DSC heating curves showing the melting temperature of PP/PS blends. b. DSC cooling curves showing the crystallization temperature of PP/PS blends.

165.5 to 160.7°C with the addition of 90 wt % PS. Similarly T_c of PP reduced from 126.6 to 117.8°C with the addition of 90 wt % PS. A careful examination reveals that when PP forms the

Table II. DSC Summary of ΔH_f , ΔH_c , T_m , T_c , and X_c of PP and T_g of PS for the PP/PS Blends

Blends	ΔH_f (J/g)	ΔH_c (J/g)	T_m (°C)	T_c (°C)	X_c (%)	T_g (PS) (°C)
PP	85.7	96.5	165.5	126.6	41.4	-
90/10	68.1	87.1	165.0	126.9	36.5	-
80/20	64.3	82.1	164.7	126.8	38.8	106
60/40	42.7	59.2	164.2	126.0	34.4	107
40/60	31.6	39.1	164.0	124.8	38.2	102
20/80	15.4	19.0	164.5	121.6	37.1	99
10/90	7.62	7.3	160.7	117.8	36.8	99
PS	-	-	-	-	-	95

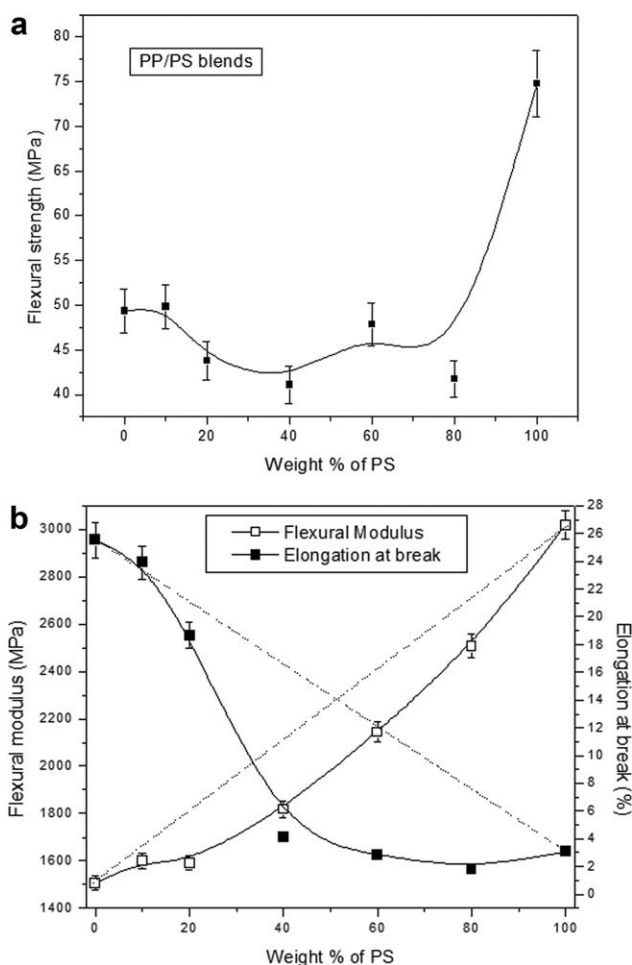


Figure 4. a. Effect of the addition of PS on the flexural strength of the PP/PS blends. b. Effect of the addition of the PS on the flexural modulus and elongation at break of the PP/PS blends.

major component in the blend, the crystallization or melting behavior of the PP was not affected by the presence of PS. On the other hand, the reduction in crystallization or melting is greatest when PP forms the dispersed phase in the blends. These results are in agreement with earlier works by Santana and Muller²⁷ and Thirtha *et al.*^{28,29} This difference in T_m and T_c of PP with respect to phase morphology is due to the difference in the nature of the spherulites formed.^{27–29}

From Table II, it is observed that, the addition of PS to PP decreased ΔH_f and ΔH_c of the blends. Thus maximum enthalpy change is associated with the melting and crystallization processes of virgin PP. The addition of amorphous PS phase decreases the melting and crystallization of the blends. The % crystallinity of the PP phase in the blends was calculated and is given in Table II. From the table, it can be seen that although the % crystallinity of the PP phase shows some fluctuations, the values were reduced for the blend system containing amorphous PS phase. This means that the regularity in arrangement or folding of PP chains into growing crystal lamellae is disturbed by the presence of the amorphous component. On the other hand, the T_g of the PS phase registered a gradual increase with the addition of PP, probably due to the fact that the crystallized

PP phase exerts some pressure on the PS phase, that can impose an increased restriction on the segmental motion of PS. This is discussed in detail in our earlier publication.²⁵ The T_g of the PS phase with respect to the blend ratio is given in Table II.

Mechanical Properties of PP/PS Blends. Flexural strength of the polymer blends is shown in Figure 4(a). From the figure, it is seen that the addition of PS to PP decreases the flexural strength and was minimum for 60/40 blends, which is followed by an increase in the flexural strength. As in the case of thermal and crystallization studies, the flexural properties are also very closely related with the blend morphology. As the concentration of the PS phase increases, the compatibility decreases and bigger droplets of PS are dispersed in the PP phase. The decrease in flexural strength is due to the poor compatibility and interfacial adhesion between the PP matrix and the PS domains which results in a weak interphase that is too weak to sustain the stress at fracture.

Flexural modulus and elongation at break (flexural testing) for the blends are shown in Figure 4(b). Flexural modulus of the polymer blends is strongly dependent on the composition and morphology. As it can be seen, the flexural modulus of blends increases with PS addition and a maximum value was obtained for neat PS phase. The compatibility does not play an important role in the case of flexural modulus since it is measured at low strain level.²³ For PP/PS system, the interface is very weak, but the phases can transfer stress at low strains, which is the reason for the increase in flexural modulus with PS addition. However, the experimental values showed deviations from the additivity line. This indicates that high degree of phase separation does not allow the stress to travel easily between the components within the system even at low strains. On the other hand, when PS is added to PP, a sharp drop in elongation at break is observed till 60/40 blends, due to the poor interfacial adhesion. After 60/40 blends, the PS phase forms the matrix, and no further decrease in the elongation in break is observed.

The effect of the blend ratio on the impact strength is shown in Figure 5. As expected, blends exhibited inferior properties.

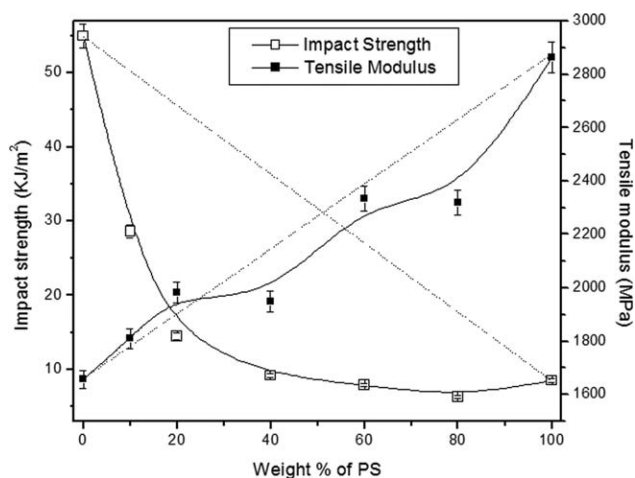


Figure 5. Effect of the addition of the PS on the impact strength and tensile modulus of the PP/PS blends.

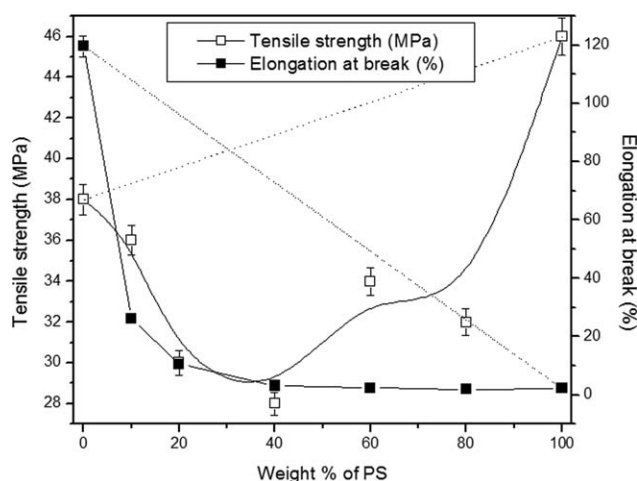


Figure 6. Effect of the addition of the PS on the tensile strength and elongation at break for the PP/PS blends.

Maximum impact strength was observed for neat PP and minimum for the neat PS system and the blends possessed an intermediate behavior. A sharp decrease in impact strength from 55 kJ/m² for the neat PP system to 15 kJ/m² at 80 wt % PP was observed, and the impact strength further decreases to 10 kJ/m² at 60 wt % PP, this is followed by a leveling off to a straight line for the remaining blends, since the PS phase forms the matrix phase. Note that in an immiscible blend, the component that forms the matrix takes on the majority of the force of the impact. From the figure it is seen that the blends possess a negative deviation from the additivity line, due to the poor compatibility between the blend components. As the concentration of one of the components increased, the impact strength decreased due to the increased incompatibility (phase separation) with composition. The impact strength was minimum for 20/80 blends.

Tensile properties also showed a similar trend. From the stress strain curves, we estimated the tensile strength, elongation at break and tensile modulus. The effect of the blend ratio on the tensile modulus is shown in Figure 5. With increase in wt % of PS in PP, a linear increase in the tensile modulus was observed. The tensile modulus of all the blends exhibit intermediate values. Tensile modulus values follow the additive rule, since it is measured at low strains.

The tensile strength and elongation at break of the PP/PS blends shown in Figure 6 reveal that the addition of PS to PP decreased these properties up to 40 wt % of PS, followed by an increase. As mentioned earlier, the increase in concentration of the PS in PP increased the incompatibility between the phases. But, beyond 40 wt % of PS in the blend, phase inversion occurred and therefore properties increased. It is important to note that the strength and toughness depend mainly on the morphology and compatibility of the blends, while the morphology and crystallinity play an important role in the modulus. Despite the fact that X_c of PP decreased slightly on blending with PS, it is not reflected in the mechanical properties. This is because phase morphology, which plays a crucial role in deciding the final mechanical properties, does not

Table III. Relative Tensile Strength and Adhesion Parameters of PP Rich Blends

Blend % PS	σ_b/σ_p	S	S'	K_b
10	0.94	1.03	1.17	0.3
20	0.79	0.96	1.15	0.67
30	0.63	0.86	1.1	0.89
40	0.73	1.15	1.5	0.53
50	0.82	1.52	2.03	0.31
Mean	0.78	1.1	1.39	0.54

depend on X_c . Thus we cannot exactly predict the final mechanical properties of the blends as a function of crystallinity.

Theoretical Modeling. Theoretical analysis of tensile strength.

In order to understand the interaction between the component polymers in PP/PS blends, predictive models were used for tensile strength data. These models include:

- i. Nielsen's first power law model [30]:

$$\frac{\sigma_b}{\sigma_p} = (1 - \phi_1)S \quad (2)$$

- ii. Nielsen's two-third power law model:³⁰

$$\frac{\sigma_b}{\sigma_p} = (1 - \phi_1^{2/3})S' \quad (3)$$

- iii. Nicolais-Narkis model:³¹

$$\frac{\sigma_b}{\sigma_p} = (1 - K_b\phi_1^{2/3}) \quad (4)$$

where σ_b represent the tensile strength of the blend and σ_p represent the tensile strength of the major component of the blend, ϕ_1 is the volume fraction of the minor phase, S and S' are Nielsen's parameters and K_b is an adhesion parameter. S and S' account for the weakness in the structure, brought about by the discontinuity in stress transfer and generation of the stress concentration at the interfaces in the case of blends. The values of S and S' are unity if there is no stress concentration effect. The value of K_b is 1.21 for spherical inclusions of the minor phase, having no adhesions. The values of relative tensile strength (σ_b/σ_p), S, S', and K_b for PP and PS rich blends are listed in Tables III and IV.

Table IV. Relative Tensile Strength and Adhesion Parameters of PS Rich Blends

Blend % PP	σ_b/σ_p	S	S'	K_b
10	0.93	1.05	1.22	0.29
20	0.71	0.91	1.12	0.79
30	0.76	1.14	1.46	0.5
40	0.75	1.34	1.77	0.43
50	0.67	1.46	1.99	0.49
Mean	0.764	1.18	1.51	0.5

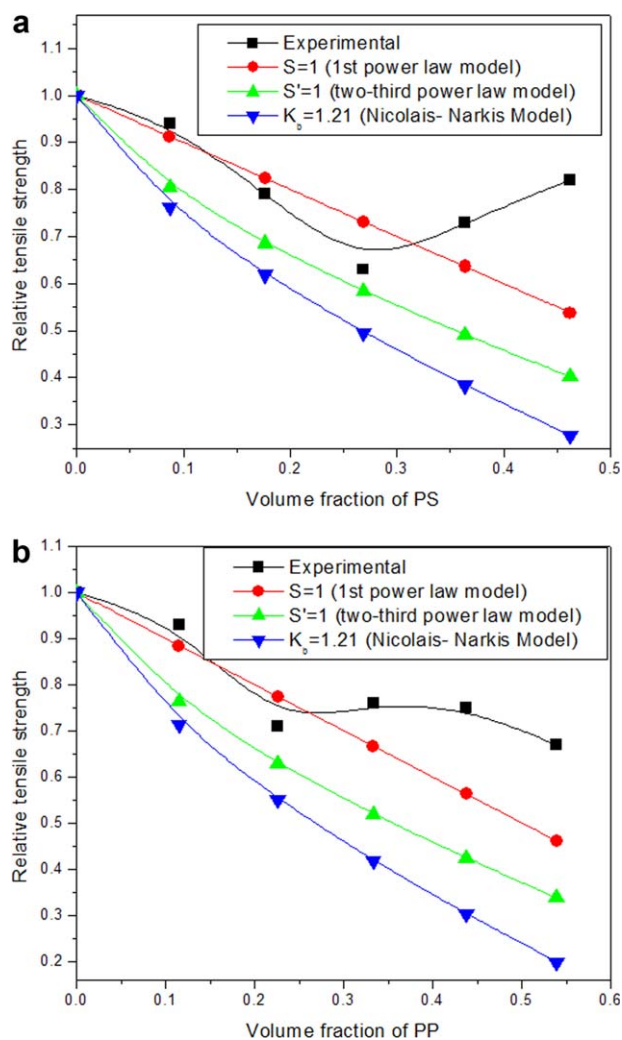


Figure 7. a, b. Plot of relative tensile strength versus volume fraction of (a) dispersed PS phase and (b) dispersed PP phase using different models. [Color figure can be viewed in the online issue, which is available at wileyonlinelibrary.com.]

From Tables III and IV, the relative tensile strength decreased with the addition of PS or PP, with respect to the pure component. The value of S and S' generally increased with the increase in relative tensile strength, however, S and S' also depend on the volume fraction of the minor component in the blend. From the tables it is observed that even though the values of S showed some irregularity, the average value is close to 1, but, the S' values are greater than 1. The value of K_b depends on the relative tensile strength. If the value of relative tensile strength is more than 1, then K_b will be negative and if the relative tensile strength is less than 1, then K_b will be positive. The positive values of K_b indicate poor adhesion between the phases.

Plots of relative tensile strength versus volume fraction of the blends, predicted from the three models, are presented in Figure 7(a,b). From Figure 7, the experimental data show some agreement with Nielsen's first power law model especially at lower concentrations of PS in PP blends and at lower concentrations of PP in PS blends. It is interesting to note that the experimen-

tal data are far better than the values predicted by the models. It is important to mention that the PP/PS blends are completely incompatible, and there exist no chemical interaction between the component polymers. However, the morphology obtained through the melt blending of PP/PS blends is capable of affecting the individual component transitions. In other words, the better tensile strength of the blend systems irrespective of the blend concentration is related to morphology and the physical interaction existing between the phases.

Theoretical analysis of Young's modulus. Modeling studies have been carried out to understand behavior of Young's modulus of the two-phase blend from the component property data. The blend models such as parallel, series, Coran, and Takayanagi models were used for predicting the Young's modulus behavior of the two phase polymer blends.

The upper bound parallel model is given by the equation:

$$M_u = \phi_1 E_1 + \phi_2 E_2 \quad (5)$$

where M_u is the modulus of the blend in the parallel model and E_1 and E_2 are tensile modulus of component 1 and 2 respectively; ϕ_1 and ϕ_2 are their corresponding volume fractions. In this model blend components are considered to be arranged parallel to one another.

The lower bound series model is given by the following equation:

$$\frac{1}{M_L} = \frac{\phi_1}{E_1} + \frac{\phi_2}{E_2} \quad (6)$$

where M_L is the modulus of the blend in the series model, and E_1 and E_2 are tensile modulus of component 1 and 2, respectively; ϕ_1 and ϕ_2 are their corresponding volume fractions. In this model blend components are considered to be arranged series to one another.

Coran's model is applicable for incompatible blends, where the properties of the blends are usually between the upper bound parallel model (M_u) and lower bound series model (M_L).³²

According to Coran's model:

$$M = f(M_u - M_L) + M_L \quad (7)$$

where M is the modulus of the blend in the Coran's model and f can vary between zero and unity.

In Coran's model the mechanical properties are between the upper bound parallel model and lower bound series model.

In the Takayanagi model³³

$$E = (1 - \lambda)E_1 + \lambda[(1 - \phi)/E_1 + (\phi/E_2)]^{-1} \quad (8)$$

where E_1 and E_2 are the moduli of the matrix phase and dispersed phase respectively, and ϕ is the volume fraction of the dispersed phase, and λ is related to the degree of series-parallel coupling.

The graphical comparison of experimental and theoretical data of tensile modulus of PP/PS blends are shown in Figure 8. The experimental curve up to 20 wt % of PS in the blends lies above the theoretical curve. However, as the concentration of PS increases the extend of phase separation increases and hence the

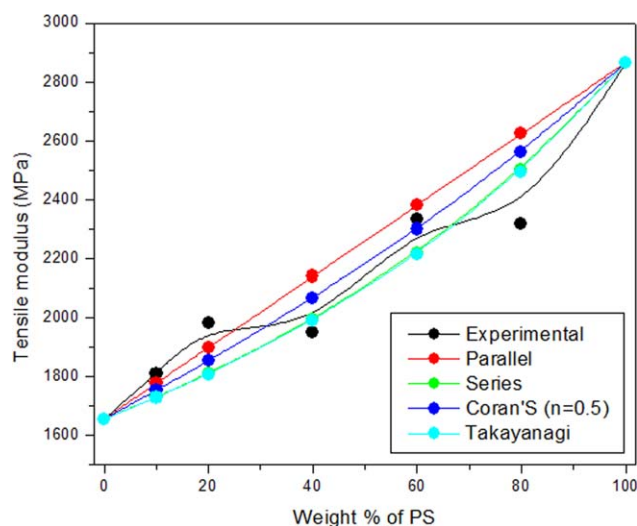


Figure 8. Plots of experimental and theoretical tensile modulus as a function of weight % of PS. [Color figure can be viewed in the online issue, which is available at wileyonlinelibrary.com.]

modulus drops slightly, but still between the upper bound parallel model and lower bound series model. Beyond 60 wt % of PS in the blends, the experimental values drop further and lag behind theoretical values.

Compatibilized Blends

Phase Morphology of the Compatibilized Blends. Scanning electron micrographs of compatibilized blends containing 2 wt % PP-g-MAH are shown in Figure 9. Matrix-droplet morphology was obtained for 90/10, 90/10 [Fig. 9(a)], 80/20 [Fig. 9(b)] and 60/40 [Fig. 9(c)] (PP/PS) blends. The PS particles are dispersed

in the PP matrix and the particle size increases with PS content. SEM micrographs revealed a more refined morphology with finer and more uniform PS domains. From our earlier studies it was found that the PP-g-MAH reacts with PS forming PP-g-PS.²⁵ The formation of PP-g-PS will modify the interface by decreasing the unfavorable interfacial interactions.^{34,35} However, the compatibilizing effect weakens at higher concentrations of PS phase.²⁵ Phase inverted structures with PP domains and PS matrix are observed for 40/60 [Fig. 9(d)] and 20/80 [Fig. 9(e)] blends. It is important to mention that for compatibilized blends containing 10 wt % PP-g-MAH, the size of the dispersed domains are larger than those of the uncompatibilized blends (not shown here), indicating the poor compatibilizing action of PP-g-MAH at higher concentrations, since most of the compatibilizer molecules may get agglomerated in the PP phase form micelles.²⁵

Mechanical Properties of Compatibilized Blends. The effect of compatibilization on the impact strength of the PP/PS blends is shown in the Figure 10. It is important to mention that the compatibilized and uncompatibilized blends showed similar trend in impact strength with respect to the blend ratio. However, a careful examination reveals an increase in impact strength with the addition of PP-g-MAH for 90/10, 80/20 blends. This means that, PP-g-MAH improved the compatibility between the blend components of these compositions. Beyond 80/20 blends, the PP-g-MAH has little influence. Blends modified with 10 wt % PP-g-MAH possessed poor impact strength irrespective of the blend composition, due to the formation of micelles resulting from the agglomeration of compatibilizer molecules in the matrix phase.

The effect of compatibilization on the tensile modulus of the PP/PS blends is shown in the Figure 11(a). The tensile modulus

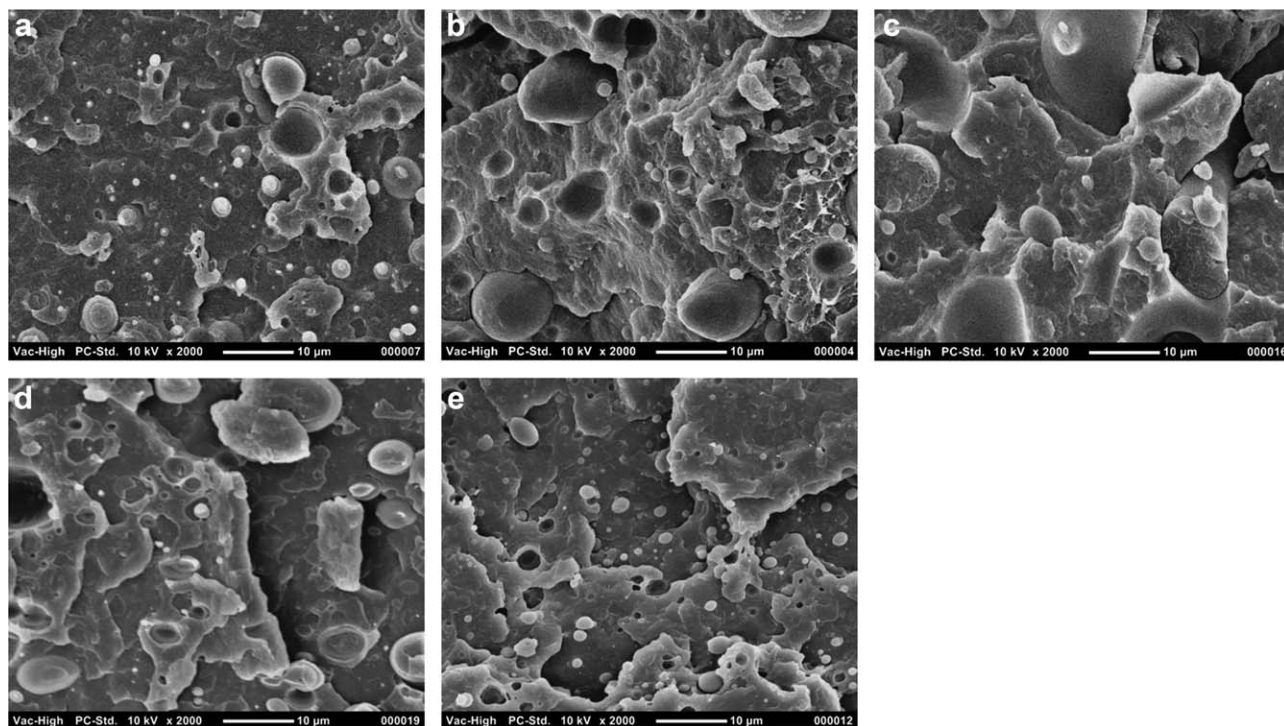


Figure 9. SEM images of PP/PS blends with 2 wt % PP-g-MAH compatibilizer.

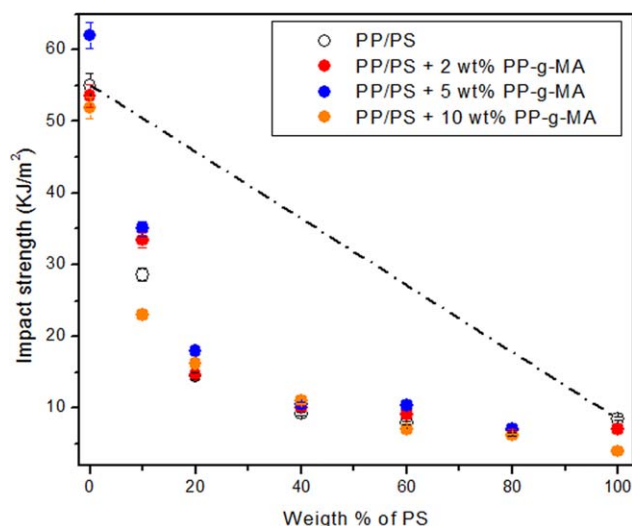


Figure 10. Effect of PS content on impact strength for blends with and without PP-g-MAH. [Color figure can be viewed in the online issue, which is available at wileyonlinelibrary.com.]

increased with the addition of PS, for compatibilized and uncompatibilized blends. Interestingly, a sharp drop in modulus is observed for PS containing 5 or 10 wt % PP-g-MAH, due to the poor compatibility of PS with PP-g-MAH. The tensile strength of the compatibilized and uncompatibilized blends is shown in Figure 11(b). From the figure it is clear that as the weight percentage of the minor phase increased, the tensile strength decreased and the minimum is reached for the blends with 80/20 and 60/40 compositions. As mentioned earlier, these results are closely related with the morphology of the blends. As the concentration of the minor phase is increased, the morphology became coarse and unstable. The tensile strength does not undergo significant change until the concentration of PS in the blends becomes 80 wt %. The addition of 2 wt % of compatibilizer has little effect on the tensile strength of the blends. However, the tensile strength of the PP/PS blends decreased with increasing amount of PP-g-MAH. These results suggest a decrease in the load-bearing-cross-section of PP with low strength PP-g-MAH.

The percentage elongation of the PP/PS blends obtained from tensile measurements for the compatibilized and uncompatibilized blends is shown in Figure 11(c). The addition of compatibilizer decreased the percentage elongation of the neat PP (120%), which is minimum for the 10 wt % addition of the PP-g-MAH (60%). However, the reduction in percentage elongation for the blend systems is little. The tensile properties did not improve with PP-g-MAH; this is due to the reduction in the properties of PP matrix by PP-g-MAH.³⁶

The effect of blend ratio on the flexural modulus of the compatibilized and uncompatibilized blends is shown in Figure 12(a). Flexural modulus increased with increasing PS content. A linear increase in flexural modulus is observed irrespective of the compatibilized and uncompatibilized blends, with increase in the amount of PS. However, the modulus of PP/PS blends decreased with PP-g-MAH. The Flexural strength for the com-

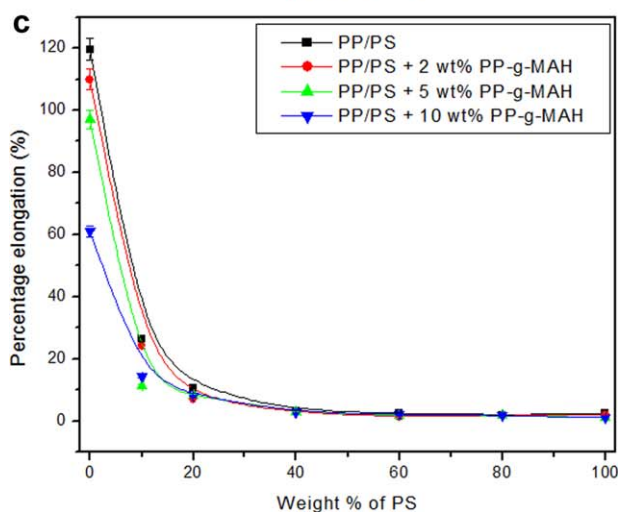
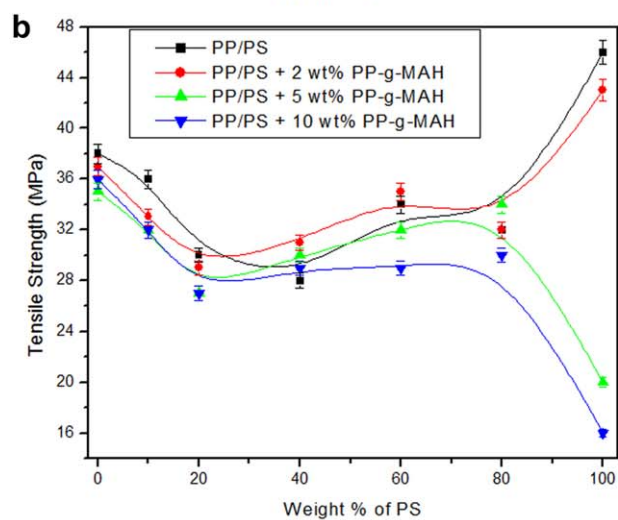
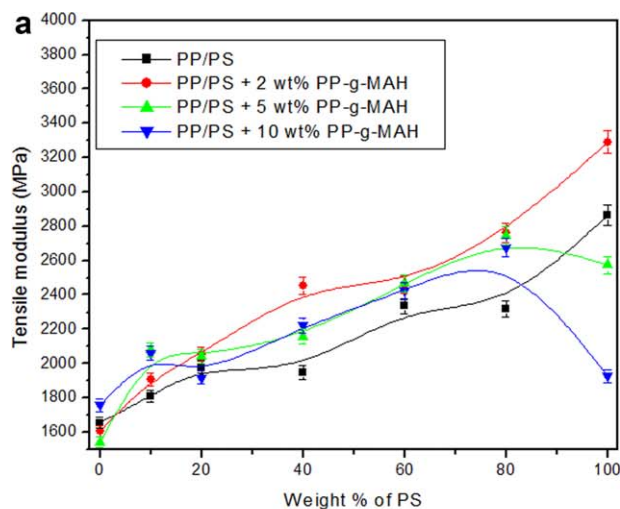


Figure 11. Effect of PS content on (a) tensile modulus, (b) tensile strength, (c) tensile elongation for blends with and without PP-g-MAH. [Color figure can be viewed in the online issue, which is available at wileyonlinelibrary.com.]

patibilized and uncompatibilized blends is shown in Figure 12(b). It is interesting to note that as the weight percentage of the minor phase increases, the flexural strength decreased

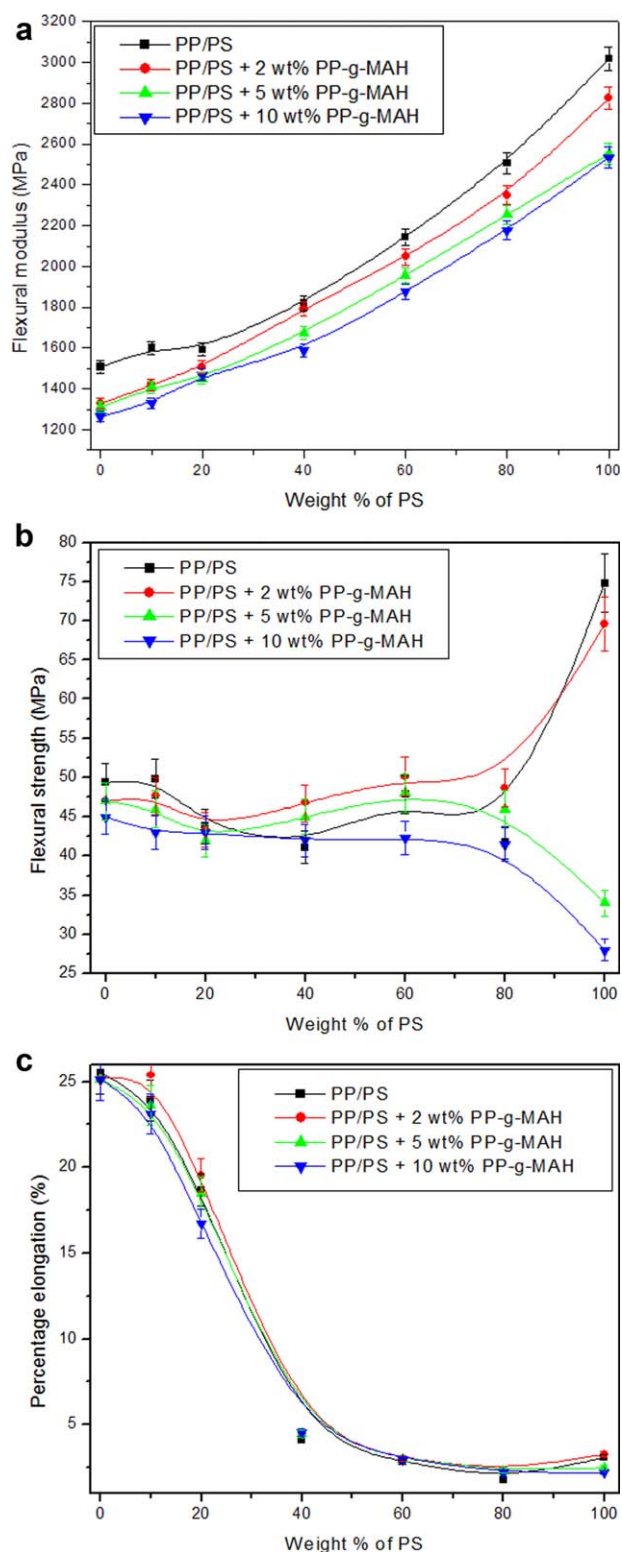


Figure 12. Effect of PS content on (a) flexural modulus, (b) flexural strength, (c) flexural elongation for blends with and without PP-g-MAH. [Color figure can be viewed in the online issue, which is available at wileyonlinelibrary.com.]

marginally and the minimum properties were obtained for 80/20 or 60/40 blends. This is in line with the phase morphology of the blends. It is important to mention that increasing

Table V. T_i , T_{max} , T_f and X_c of 80/20 and 20/80 Compatibilized Blends

Samples (PP/PS)	T_i (°C)	T_{max} (°C)	T_f (°C)	X_c (%)
80/20 blend	409	442	493	38.8
80/20 + 2 wt % PP-g-MAH	408	441	477	42.9
80/20 + 5 wt % PP-g-MAH	408	445	480	38.2
80/20 + 10 wt % PP-g-MAH	408	444	483	49.2
20/80 blend	407	435	451	37.1
20/80 + 2 wt % PP-g-MAH	393	414	447	43.1
20/80 + 5 wt % PP-g-MAH	393	412	450	45.1
20/80 + 10 wt % PP-g-MAH	396	412	450	53.7

amount of PP-g-MAH decreased the flexural strength, irrespective of the blend composition. The percentage elongation decreased with increase in the amount of PS in the blends [Figure 12(c)]. The addition of compatibilizer has little effect on the variation of percentage elongation. A careful examination reveals that, 2 wt % of the compatibilizer increased the % elongation of the blends, but at higher concentrations of compatibilizer, the % elongation is decreased.

Thermal Properties of Compatibilized Blends. To understand the thermal and crystallization behavior of the polymer blends 80/20 and 20/80 blends were selected and the effect of PP-g-MAH on the thermal and crystallization behavior are shown in Table V. For 80/20 blends, most of the PP-g-MAH are located at the interface between the blend components. Hence the thermal stability was not much affected by the addition of PP-g-MAH. Note that the values for T_i , T_{max} , and T_f remain the same irrespective of the PP-g-MAH content. For 20/80 blends PP-g-MAH may get agglomerated in the PP phase, moreover there exists poor compatibility between the PS phase and the compatibilizer and hence poor thermal properties for compatibilized blends with PS matrix phase. The % crystallinity calculated from the DSC thermogram is given in Table V. From the table, it can be seen that irrespective of the composition, addition of compatibilizer increases the % crystallinity, which is maximum with 10 wt % PP-g-MAH. As mentioned in the previous section, the PP-g-MAH molecules may get dispersed in both the PP and PS phase; especially at higher compatibilizer concentration. Therefore, the increase in % crystallinity could be due to nucleating action of PP-g-MAH in PP.

CONCLUSIONS

The present research work dealt with the investigation of the effects of blend ratio and compatibilization on the morphology, thermal, crystallization and mechanical properties of PP/PS blends. Thermogravimetric studies revealed that blend ratio has significant impact on the thermal stability of the polymers. Addition of PS into PP decreased the thermal stability of the blends significantly, the blend possessed intermediate stability. Phase morphology was found to be one of the decisive factors that affected the thermal stability since the thermal stability depends on the stability of the matrix phase. The melting and crystallization behaviors of the blends revealed that blending

has significant effect on the melting and crystallization properties of PP. Crystallization and melting temperatures of PP were found to be approximately 165.5 and 126.6°C, respectively and these values decreased gradually by the addition of PS. The tensile strength, flexural strength, elongation at break, and impact strength decreased by blending PS with PP. The compatibilizer is found effective for stabilizing the morphology and improving the impact strength for blends, however irregularities in other mechanical properties are observed with respect to the neat blend. Finally the thermal properties show some variations by the addition of PP-g-MAH. For blends with PP matrix thermal stability was retained by the addition of PP-g-MAH, but for blends with PS matrix, thermal stability was decreased with increasing PP-g-MAH content. Percentage crystallinity was increased with PP-g-MAH showing the efficiency of PP-g-MAH in increasing the crystallinity of PP phase.

ACKNOWLEDGMENTS

J.P. acknowledges the Department of Science and Technology, Government of India, for financial support under an Innovation in Science Pursuit for Inspired Research (INSPIRE) Faculty Award (contract grant number IFA-CH-16). N.H. acknowledges the funding from Australian Academy of Science under the Australia India Early Career Research Fellowship program.

REFERENCES

1. Omonov, T. S.; Harrats, C.; Moldenaers, P.; Groeninckx, G. *Polymer* **2007**, *48*, 5917.
2. Omonov, T. S.; Harrats, C.; Groeninckx, G.; Moldenaers, P. *Polymer* **2007**, *48*, 5289.
3. Hlavatá, D.; Horák, Z.; Hromádková, J.; Lednický, F.; Pleska, A. *J. Polym. Sci. Part B: Polym. Phys.* **1999**, *37*, 1647.
4. Macaúbas, P. H. P.; Demarquette, N. R. *Polymer* **2001**, *42*, 2543.
5. Halimatudahliana; Ismail, H.; Nasir, M. *Polym. Test.* **2002**, *21*, 263.
6. Adewole, A. A.; Denicola, A.; Gogos, C. G.; Mascia, L. *Plastic. Rubber C* **2000**, *29*, 70.
7. Halimatudahliana; Ismail, H.; Nasir, M. *Polym. Test.* **2002**, *21*, 163.
8. Waldman, W. R.; De Paoli, M. *Polym. Degrad. Stab.* **2008**, *93*, 273.
9. Diaz, M. F.; Barbosa, S. E.; Capiati, N. *J. Polymer* **2005**, *46*, 6096.
10. Li, J.; Li, H.; Wu, C.; Ke, Y.; Wang, D.; Li, Q.; Zhang, L.; Hu, Y. *Eur. Polym. J.* **2009**, *45*, 2619.
11. Kim, J.; Kwak, J.; Kim, D. *Polym. Adv. Technol.* **2003**, *14*, 58.
12. Adewole, A. A.; Denicola, A.; Gogos, C. G.; Mascia, L. *Adv. Polym. Technol.* **2000**, *19*, 180.
13. Hung, C.; Chuang, H.; Chang, F. *J. Appl. Polym. Sci.* **2008**, *107*, 831.
14. Baker, W. E.; Saleem, M. *Polym. Eng. Sci.* **1987**, *27*, 1634.
15. Saleem, M.; Baker, W. E. *J. Appl. Polym. Sci.* **1990**, *39*, 655.
16. Majumdar, B. and Paul, D. R. In *Polymer Blends: Formulation*; Pauland, D. R., Bucknall, C. B., Eds.; Wiley-Interscience: New York, **2000**; Vol. 1, Chapter 17, p 539.
17. Tiwari, R. R.; Paul, D. R. *Polymer* **2011**, *52*, 1141.
18. Elias, L.; Fenouillot, F.; Majeste, J. C.; Cassagnau, Ph. *Polymer* **2007**, *48*, 6029.
19. Al-Saleh, M. H.; Sundararaj, U. *Eur. Polym. J.* **2008**, *44*, 1931.
20. Santra, R. N.; Mukunda, P. G.; Nando, G. B.; Chaki, T. K. *Thermochim. Acta* **1993**, *219*, 283.
21. Jose, S.; Aprem, A. S.; Francis, B.; Chandy, M. C.; Werner, P.; Alstaedt, V.; Thomas, S. *Eur. Polym. J.* **2004**, *40*, 2105.
22. Horak, Z.; Fort, V.; Hlavata, D.; Lednický, F.; Vecerka, F. *Polymer* **1996**, *37*, 65.
23. Jose, S.; Thomas, S.; Biju, P. K.; Karger-Kocsis, J. *J. Polym. Res.* **2013**, *20*, 1.
24. Brostow, W.; Holjevac Grguric, T.; Olea-Mejia, O.; Pietkiewicz, D.; Rek, V. *e-Polymers* **2008**, *8*, 364.
25. Parameswaranpillai, J.; Joseph, G.; Chellappan, R. V.; Zahakariah, A. K.; Hameed, N. *J. Polym. Res.* **2015**, *22*, 641.
26. Wildes, G.; Keskkula, H.; Paul, D. R. *Polymer* **1999**, *40*, 5609.
27. Santana, O. O.; Muller, A. *J. Polym. Bull.* **1994**, *32*, 471.
28. Thirtha, V.; Lehman, R.; Nosker, T. *Polym. Eng. Sci.* **2005**, *45*, 1187.
29. Thirtha, V.; Lehman, R.; Nosker, T. *J. Appl. Polym. Sci.* **2008**, *107*, 3987.
30. Nielsen, L. E. *J. Appl. Polym. Sci.* **1966**, *10*, 97.
31. Nicolais, L.; Narkis, M. *Polym. Eng. Sci.* **1971**, *11*, 194.
32. Coran, A. Y.; Patel, A. In *Handbook of Elastomers – New Developments and Technology*; Bhowmick, A. K., Stephens, H. L., Eds.; Marcel Dekker: New York, **1988**; p 249.
33. Dickir, R. A. *J. Appl. Polym. Sci.* **1973**, *17*, 45.
34. Caporaso, L.; Iudici, N.; Oliva, L. *Macromolecules* **2005**, *38*, 4894.
35. Dorazio, L.; Guarino, R.; Mancarella, C.; Martuscelli, E.; Cecchin, G. *J. Appl. Polym. Sci.* **1997**, *65*, 1539.
36. Kim, D. H.; Fasulo, P. D.; Rodgers, W. R.; Paul, D. R. *Polymer* **2007**, *48*, 5308.